

Large Model Based Referring Camouflaged Object Detection

Shupeng Cheng¹ Ge-Peng Ji² Pengda Qin³ Deng-Ping Fan⁴ Bowen Zhou¹ Peng Xu¹

¹Department of Electronic Engineering, Tsinghua University

²School of Computing, Australian National University

³Alibaba Group

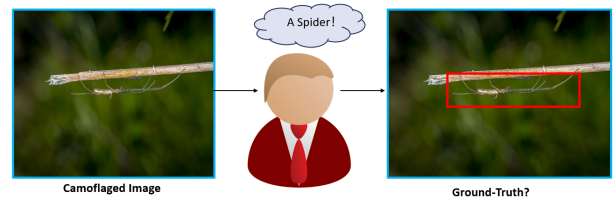
⁴Nankai International Advanced Research Institute, Nankai University

chengsp20@mails.tsinghua.edu.cn gepengai.ji@gmail.com pengda.qpd@alibaba-inc.com

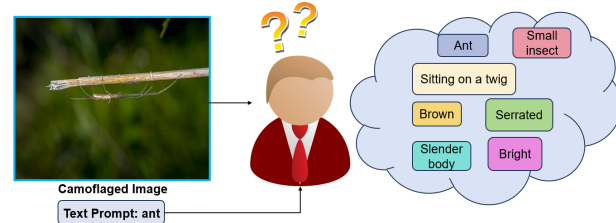
dengpfan@gmail.com zhoubowen@tsinghua.edu.cn peng_xu@tsinghua.edu.cn

Abstract

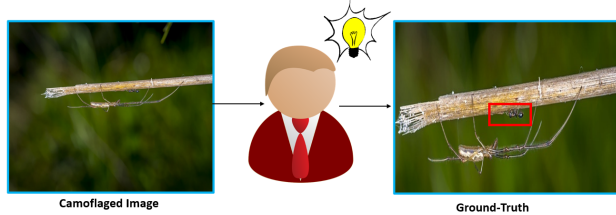
Referring camouflaged object detection (Ref-COD) is a recently-proposed problem aiming to segment out specified camouflaged objects matched with a textual or visual reference. This task involves two major challenges: the COD domain-specific perception and multi-modal reference-image alignment. Our motivation is to make full use of the semantic intelligence and intrinsic knowledge of recent Multimodal Large Language Models (MLLMs) to decompose this complex task in a human-like way. As language is highly condensed and inductive, linguistic expression is the main media of human knowledge learning, and the transmission of knowledge information follows a multi-level progression from simplicity to complexity. In this paper, we propose a large-model-based **Multi-Level Knowledge-Guided** multimodal method for Ref-COD termed **MLKG**, where multi-level knowledge descriptions from MLLM are organized to guide the large vision model of segmentation to perceive the camouflage-targets and camouflage-scene progressively and meanwhile deeply align the textual references with camouflaged photos. To our knowledge, our contributions mainly include: (1) This is the first time that the MLLM knowledge is studied for Ref-COD and COD. (2) We, for the first time, propose decomposing Ref-COD into two main perspectives of perceiving the target and scene by integrating MLLM knowledge, and contribute a multi-level knowledge-guided method. (3) Our method achieves the state-of-the-art on the Ref-COD benchmark outperforming numerous strong competitors. Moreover, thanks to the injected rich knowledge, it demonstrates zero-shot generalization ability on uni-modal COD datasets. **We will release our code soon.**



(a) Ignore the truly camouflaged object at first glance



(b) Leverage multi-level knowledge given the text prompt



(c) Perceive the camouflaged object under the guidance of multi-level knowledge

Figure 1. Our motivation: Given a camouflaged photo with a text reference, persons can leverage their inherent multi-level knowledge that is beyond the visual domain to enhance the recognition of subtly camouflaged objects that are prone to be overlooked. Best viewed in colour.

1. Introduction

Camouflaged object detection (COD) [9] is a vision topic that is widely studied with diverse real-world applications, including rare species discovery, healthcare (e.g., automatic diagnosis of colorectal polyps [17]), and agriculture (e.g.,

pest identification [32]). In 2023, Zhang *et al.* [66] enhanced this pure vision task further by proposing a multi-modal setting, termed referring camouflaged object detection (Ref-COD). This novel task aims to tackle a kind of practical scenarios where the models segment out specified camouflaged objects based on a textual or visual reference. Its goal is to make the process of camouflaged visual perception more orientable and efficient. In this paper, we focus on the scenarios that use textual reference, *e.g.*, class label of the target object.

1.1. Motivation

However, Ref-COD is a challenging problem and even the large vision models fail to solve it well [21]. We do have to consider at least two major problems. (1) It is challenging for the models to perceive the complex patterns in the camouflaged scenes. Even for the human eyes, it is not easy to recognize objects with camouflage properties from a camouflage scene. As illustrated in Figure 1, if a person is presented with a text prompt/reference, that person is likely to combine some prior knowledge other than visual information to solve the Ref-COD problem. In some sense, this task goes beyond visual perception, thus it is natural for us to consider injecting some domain knowledge into the model to enhance its perception ability. (2) The textual references make the models need to handle the cross-modal alignment between the camouflaged photo and its textual reference. If the textual references are too short and abstract to be overly intricate for the models and the models have not seen the relevant corpus during the pre-training, the cross-modal alignment will be more difficult. For instance, if the textual reference is a class label [bird], it is easy for the models to associate this concept with the visual attributes of various birds, as birds are common in the training corpus such that the models have built-in knowledge of birds and their habitat scenes. However, let us imagine a difficult case that if the textual reference is a rare species [platypus], which is infrequent in the training corpus and even the real world. As a result, the models do not have any knowledge of platypuses and their habitat scenes to align the reference word [platypus] to the corresponding camouflaged photos of platypuses. Considering this limitation, we would use comprehensible/rich natural language to explain and enhance the abstract textual references for Ref-COD. This would mainly have two benefits: (a) rich natural language will bring extra knowledge for the models to inject unseen patterns. (b) and meanwhile make it easier for the models to align the cross-modal inputs.

Nowadays, AI research has entered the era of large models (LM). New research opportunities are emerging. Thanks to the multimodal capabilities of Transformers [55], we see a trend that various LMs (*e.g.*, large language models (LLMs) [27, 50], multimodal large models [29, 30], large

vision models [11, 23]) have achieved great success on numerous applications. Given the superior semantic intelligence and rich knowledge of LMs, in this paper, we would like to make the first attempt to explore LM knowledge to alleviate the aforementioned task-specific challenges of Ref-COD, and meanwhile implement a solution with interpretability.

1.2. Method Overview

Based on the above motivations and motivated by LM’s fruitful applications on complex task decomposition [24, 51], our idea is to make full use of the semantic intelligence and intrinsic knowledge of MLLMs to decompose this complex task in a human-like way. Specifically, we would decompose the complex logic of Ref-COD into two main perspectives, perceiving camouflage-targets and camouflage-scene progressively. This could guide the model to explicitly figure out two questions. The first question is that *what specific objects it needs to separate*, and the second question is that *what kind of camouflaged scene it handles*. We believe that effectively addressing these two issues can greatly enhance the interpretability of the model. In this paper, we propose a MLLM-based **M**ulti-**L**evel **K**nowledge-**G**uided multimodal method for Ref-COD termed MLKG, where multi-level knowledge descriptions from the popular MLLM LLaVA-1.5 [29] are organized to guide the large vision model SAM [23] to perceive the camouflage-target and camouflage-scene progressively and meanwhile deeply align the textual references with camouflaged photos.

1.3. Contributions

To our knowledge, our contributions can be mainly summarized as follows.

(1) This is the first work to explore the powerful capabilities of MLLMs to guide the task of Ref-COD and COD, which naturally brings better interpretability.

(2) We, for the first time, propose decomposing Ref-COD into two main perspectives of perceiving the camouflage-target and camouflage-scene by integrating MLLM knowledge to guide the model to explicitly figure out what specific objects it needs to separate from what kind of camouflage scene, and contribute a multi-level knowledge-guided method.

(3) Our method achieves the state-of-the-art on the Ref-COD benchmark outperforming numerous strong competitors. Moreover, thanks to the injected rich knowledge, it demonstrates zero-shot generalization ability on uni-modal COD datasets.

2. Related Work

2.1. Camouflaged Object Detection

The field of COD has developed rapidly in recent years. As discussed in survey [9], the recent methods can be categorized into three architectures. (1) *Multi-stream framework* utilizes various feature flows for understanding camouflaged scenes. Those methods are exemplified by generating pseudo-depth maps [52], calculating pseudo-edge uncertainty [22], employing an adversarial learning paradigm [28] or a frequency enhancement stream [68], and exploiting multi-scale [40] and multi-view [67] inputs or ensemble backbones [46]. (2) *Bottom-up/top-down framework*, also known as the UNet-shaped framework [44], generates segmentation masks through sequential encoding and decoding procedures. This framework is the most popular in the COD community, with numerous variants such as the method utilizing a coarse-to-fine refinement strategy [47] and its enhancement versions [7, 8, 10, 15, 16, 37, 38, 54, 59] with a deeply-supervised strategy [26]. (3) *Branched framework* follows a single-input-multiple-output design and is typically formulated as a multi-task learning pipeline. For example, this framework incorporates auxiliary tasks such as confidence estimation [28, 31, 56, 64], target localization/ranking [34, 35], category prediction [25], depth estimation [52, 53], boundary detection [18, 49, 63, 69, 70, 72], and texture exploration [20, 71]. In this paper, we focus on the referring camouflaged object detection (Ref-COD) that is a multimodal task. The models aim to segment out specified camouflaged objects matched with a textual reference.

2.2. Knowledge Augmented Methods

The incorporation of high-quality knowledge guidance has been proven to play a crucial role in improving the performance of downstream tasks. Plenty of conventional approaches rely on explicit knowledge injection [4, 39, 45, 60, 62]. KERL [2] introduces a knowledge-embedded image recognition method, where rich visual concepts in the form of knowledge graph are leveraged to improve performance. MuRAG [3] resorts to the external knowledge corpus to solve question-answering tasks by retrieving related multimodal knowledge. As model size continues to increase, large models [27, 50, 61] exhibit exponential growth in their ability of knowledge capacity and reasoning. Recent Multimodal Large Language Models (MLLMs) [30, 57] are able to generate rational analysis when given images and textual instructions. LLaVA-1.5 [29] properly aligns large-scale vision encoder with LLM and achieves the state-of-the-art on various multimodal understanding tasks, where the understanding of given images can be expressed as language just like humans. Based on this, the proposed method treats MLLMs as a high-quality knowledge generator to provide multi-level knowledge for Ref-COD and COD.

3. Methodology

3.1. Formulation

We assume a training dataset \mathbf{X} in the form of N camouflaged photos: $\mathbf{X} = \{\mathbf{X}_i = (\mathbf{p}_i^{camo}, t_i^{ref})\}_{i=1}^N$. Each camouflaged photo $\mathbf{p}_i^{camo} \in \mathbb{R}^{3 \times H \times W}$ has a textual class label t_i^{ref} of the target objects, where H and W denote the height and width of \mathbf{p}_i^{camo} . There may be multiple camouflaged objects in \mathbf{p}_i^{camo} , and we need to segment out the specific objects by matching the targets provided by the reference t_i^{ref} . Thus, in Ref-COD task, we aim to learn a multimodal mapping $\mathcal{M} : \mathbf{X}_i \rightarrow \mathbf{M}_i^{seg}$ to output a binary mask $\mathbf{M}_i^{seg} \in \{0, 1\}^{H \times W}$ that can segment out the camouflaged objects from \mathbf{p}_i^{camo} , which are matching its reference t_i^{ref} .

3.2. Pipeline Overview

In this work, we propose a large model based multi-level knowledge-guided multimodal method for Ref-COD, termed MLKG. As illustrated in Figure 2, our pipeline consists of five components:

(1) **Visual Encoder** takes in the camouflaged photo \mathbf{p}_i^{camo} and produces visual representation that is transmitted to the visual decoder;

(2) **Visual Decoder** synchronously receives visual representation and domain knowledge from the visual encoder and knowledge injector respectively, and outputs the segmentation mask \mathbf{M}_i^{seg} to predict the specific camouflaged targets matched with the reference t_i^{ref} ;

(3) **Knowledge Factory** is a multimodal large language model that translates the target reference t_i^{ref} as multi-level knowledge descriptions and transmits them to the knowledge encoder;

(4) **Knowledge Encoder** is a text encoder that takes in the multi-level knowledge from the knowledge factory and encodes each level of knowledge into a vector that is passed into the knowledge injector;

(5) **Knowledge Injector** receives the outputs of the knowledge encoder, and completes two signal processing steps: a) It selects and fuses the encoded representation of multi-level knowledge received from the knowledge encoder, b) The selected and fused knowledge is input to the visual decoder after cross-modal alignment with the visual decoder’s representation space.

Our pipeline is trained in an end-to-end manner with a binary cross entropy (BCE) loss connected to our visual decoder. In particular, we use the configuration of a large vision model SAM [23] to implement our visual encoder and decoder. The text encoder of CLIP [43] is adopted as our knowledge encoder. In the following sections, we will describe our knowledge factory and injector in detail. See Section 4 for more implementation details of all our components.

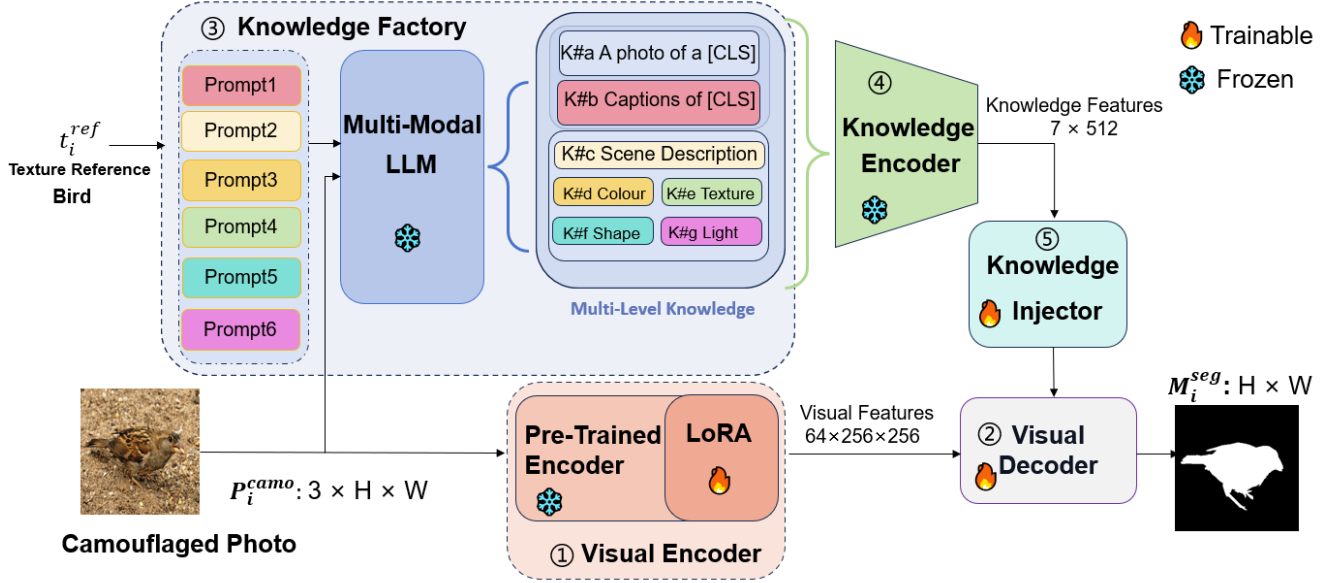


Figure 2. Pipeline of our MLKG method. Best viewed in colour.

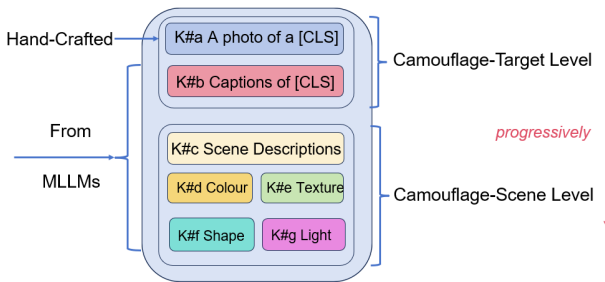


Figure 3. Illustration of our multi-level knowledge. Best viewed in colour.

3.3. Knowledge Factory

In this paper, our textual target reference t_i^{ref} is a textual class label. We design a multi-level knowledge structure to help the model to decompose Ref-COD task in a human-like manner, perceiving camouflage-targets and camouflage-scene. This could guide the model to explicitly figure out two questions **Q1**: what specific objects it needs to separate, and **Q2**: what kind of camouflaged scene it handles. Moreover, we would make full use of the semantic intelligence and intrinsic knowledge of MLLMs to help the model catch up on knowledge related to these two problems.

For **Q1**, the model requires a clear category name and may need to learn some knowledge of the morphological information or physical characteristics of the specific kind of objects matched with the target reference, disregarding

background related interference information. For instance, if the target is a kind of animal, it would not be good for the model to consider the knowledge of their habitat to solve **Q1**.

For **Q2**, it would be necessary for the model to learn the knowledge of the camouflaged scene to know which attributes in the scene can cause the camouflage effect of the particular objects, *e.g.*, colour, texture, shape, lighting.

Based on the above analysis, we propose a multi-level knowledge guidance (illustrated in Figure 3), *i.e.*, camouflage-target level and camouflage-scene level, which have both hand-crafted texts and detailed language descriptions extracted from MLLMs. As listed in Table 1, we designed a series of prompts to retrieve multiple knowledge from MLLMs to organize our domain-specific knowledge.

Camouflage-Target Level has two knowledge components: **K#a** (knowledge a): a hand-crafted text template ‘A photo of a [CLS]’ that follows the recently good practice of image classification [43] to let the model know what category it needs to perceive. **K#b**: a detailed description of the morphological information and/or physical characteristics of the specific target, which is extracted from a MLLM by our Prompt 1 (P#1).

Camouflage-Scene Level provides multiple (from global to fine-grained) knowledge of the camouflaged scene, including five components: **K#c** describes the full scene from a global perspective. **K#d**, **K#e**, **K#f**, and **K#g** respectively offer the fine-grained scene description by focusing on colour, texture, shape, and lighting properties. Knowledge **K#c** - **K#g** are extracted from a MLLM via us-

Table 1. Our hand-crafted prompts for multimodal LLM. P#1 is a text prompt, and others are used as multimodal prompts with image inputs. ‘[CLS]’ denotes a placeholder for the class name. Double quotes are used to direct the large model to focus on the key words.

| Num | Content |
|-----|--|
| P#1 | This is a picture of a [CLS] hidden in the background, please give me a brief description based only on the morphological information of a general [CLS] (Only describe physical characteristics, do not need to describe life habits and so on). No more than 50 words. |
| P#2 | Please use detailed language to describe the entire scene in the given image of a [CLS]. No more than 30 words. |
| P#3 | Within this scene, how does the [CLS] blend in the environment? Please describe it from the perspective of “colour” in one sentence. |
| P#4 | Within this scene, how does the [CLS] blend in the environment? Please describe it from the perspective of “texture” in one sentence. |
| P#5 | Within this scene, how does the [CLS] blend in the environment? Please describe it from the perspective of “shape” in one sentence. |
| P#6 | Within this scene, how does the [CLS] blend in the environment? Please describe it from the perspective of “environment lighting condition” in one sentence. |

ing our prompts P#2 - P#6, respectively.

After our multi-level knowledge is organized, the knowledge factory module outputs it to the knowledge encoder, as demonstrated in Figure 2. The knowledge encoder is responsible for transferring knowledge from the linguistic domain to embedding space, via encoding each level of knowledge into a vector that is passed into the knowledge injector.

3.4. Knowledge Injector

As the aforementioned, our knowledge injector receives the outputs of the knowledge encoder, and completes two signal processes: (a) selecting and fusing the multi-level knowledge and (b) aligning the knowledge with the visual patterns.

(a) The knowledge injector selects and fuses the encoded representation of multi-level knowledge received from the knowledge encoder. For clear interpretability, we designed a weighted fusion strategy to select and fuse the multiple encoded knowledge. As demonstrated in Figure 4, our knowledge injector adapts the encoded knowledge to inter-level and intra-level selection and fusion, to generate well-

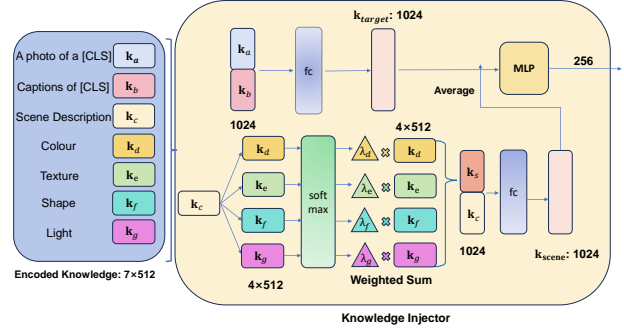


Figure 4. Illustration of our knowledge injector. The numbers denote the vector/matrix shapes. ‘fc’ means fully connected layer. Best viewed in colour.

integrated guidance for the visual decoder. Specifically, knowledge $K\#a - K\#g$ are encoded into seven 512d vectors, denoted as $k_a - k_g$. The encoded vectors k_a and k_b of camouflage-target level knowledge $K\#a$ and $K\#b$ are concatenated as a 1024d vector, followed by a 1024×1024 fully connected layer, resulting in a 1024d vector k_{target} . For camouflage-scene level knowledge $K\#c - K\#g$, we employ a weighted fusion strategy. $K\#c$ globally describes the scene of the image, while $K\#d - K\#g$ separately describes the camouflage scene from the perspectives of colour, texture, shape, and light. The proportions of these four aspects vary for different camouflaged photo instances. Therefore, we use the respective similarity between k_c and $k_d - k_g$ to determine the knowledge proportions. We compute the dot product between k_c and $k_d - k_g$ to obtain four affinity values. After applying the softmax function, these values yield weights $\lambda_d - \lambda_g$. By performing a weighted sum on $k_d - k_g$ using $\lambda_d - \lambda_g$, we obtain a new 512d vector k_s . Concatenating k_s and k_c , and passing them through a 1024×1024 fully connected layer, we obtain a 1024d vector k_{scene} . Finally, the average of k_{target} and k_{scene} serves as the guidance output by the knowledge injector, which is then injected into the visual decoder. All activation functions for the mentioned fully connected layers above use GELU [13]. (b) The selected and fused knowledge is input to the visual decoder after cross-modal alignment with the visual decoder’s representation space. In particular, as stated in our motivation, the injected multi-level knowledge makes it easier for the models to align the cross-modal gaps between the camouflaged photos and knowledge. Thus, our knowledge injector uses an MLP to project the knowledge into our visual decoder, no need to consider other more complex adapter networks. Then, the visual decoder synthetically perceives both the visual patterns and knowledge to predict the target masks as the final outputs.

For instance, we randomly select an example from the class Mockingbird in our testing set, and extract multi-level



Figure 5. A randomly-selected camouflaged photo. In the center of the picture, a bird stands on a stake. Best viewed in colour.

knowledge from MLLM. See Figure 5 and Table 2. In this example, the weights corresponding to ‘colour’, ‘texture’, ‘shape’, and ‘light’ are 0.30, 0.25, 0.27, and 0.18, respectively. This implies that the mockingbird in the image primarily relies on colour to achieve camouflage, because it closely matches the environment. This aligns well with the intuitive perception.

Here, we would state a minor contribution of ours. As stated earlier, our visual encoder and decoder are implemented by a SAM. However, SAM decoder natively is aligned with the short texts on the category level and its source code for this vision-text alignment has never been released. In our work, we reproduced this part of the code and deeply aligned SAM with our complex and structured texts/knowledge. Compared with the shallow alignment of the original SAM, ours is a more deeply aligning practice. This takes the cross-modal alignment for SAM a step forward. To our knowledge, our work contributes the first SAM-based Ref-COD solution.

4. Experiments

4.1. Datasets

R2C7K [66] is a recently proposed large-scale dataset for referring camouflaged object detection task. It consists of 2987 camouflaged images for training and 1987 images for testing. In COD field, there are four popular datasets: a) CAMO [25] has 1000 camouflaged images for training and 250 for testing. b) CHAMELEON [7] consists of 76 images obtained through a Google search for ‘camouflaged animals’ and is solely used for testing purposes. c) NC4K [34] is currently the largest dataset used to test COD models and consists of 4121 camouflaged images in natural and artificial scenes. d) COD10K [8] includes 5066 camouflaged images, with 3040 for training and 2026 for testing. In our experiment, we use R2C7K [66] and COD10K [8] to per-

Table 2. Our MLLM based multi-level knowledge for the randomly-selected example in Figure 5.

| Knowledge Category | Content |
|--------------------|---|
| K#a | ‘A photo of a Mockingbird.’ |
| K#b | ‘A small bird with a gray body, white underbelly, and black wings. It is perched on a fence post.’ |
| K#c | ‘A mockingbird perched on a fence post.’ |
| K#d | ‘The mockingbird blends in with the environment by perching on a wooden fence post, which is a part of the natural surroundings.’ |
| K#e | ‘The mockingbird’s brown and white feathers blend in with the surrounding trees and fence, creating a natural texture that makes it difficult to distinguish from its surroundings.’ |
| K#f | ‘The mockingbird blends in the environment by perching on a wooden fence post, which is shaped like a T, and is surrounded by trees and a car.’ |
| K#g | ‘The lighting condition in the scene further enhances the bird’s blending in, as the sunlight filtering through the trees casts a warm, natural glow on the bird and its surroundings.’ |

form Ref-COD training and testing. Furthermore, we evaluate the zero-shot generalization ability of our method on CHAMELEON, NC4K, and the testing set of CAMO.

4.2. Protocols and Metrics

Following previous standard protocols in COD, we adopt four widely used metrics to evaluate our method, *i.e.*, structure-measure (S_m) [5], adaptive E-measure (αE) [6], weighted F-measure (F_β^w) [36], and mean absolute error (M) [42]. Specifically, S_m [5] measures both object-aware similarity and region-aware similarity; αE [6] considers both local and global similarity between two prediction masks; F_β^w [36] is an exhaustive measure of both recall and precision; M [42] is the absolute difference between the prediction mask and the ground-truth.

4.3. Implementation Details

We implement our method using the PyTorch [41] library. Specifically, we choose the image encoder and decoder of SAM [23] as our visual encoder and decoder, respectively. The parameters are initialized with SAM’s public checkpoint ViT-H [23]. SAM encoder is a heavy network, thus we fine-tune it with LoRA [14] to preserve its powerful representational capacity while reducing computational complexity. We choose CLIP text encoder as our knowledge encoder, and its parameters are initialized with CLIP’s public checkpoint ViT-B/16 [43] and are frozen during our training. SGD with momentum 0.9 is used as our optimizer. Our learning rate is initially set to 5e-3 and decays following the cosine learning rate strategy. All our experiments are conducted on an NVIDIA GeForce RTX 3090 GPU.

4.4. Result Analysis

To demonstrate the effectiveness of our method, we compare it with numerous strong competitors in COD field. In Tables 3 and 4, we observed that our model obviously outperforms the existing competitors in three key metrics: S_m , F_β^w , and M . Although our method may sometimes not be optimal in the indicator of αE , the overall performance of

Table 3. Quantitative comparison on Ref-COD benchmark R2C7K [66] against COD methods and their Ref-COD versions. ‘RefT’ means ‘with textual reference’. ‘Single-Obj’ denotes the scene of a single camouflaged object; ‘Multi-Obj’ denotes the scene of multiple camouflaged objects; ‘Overall’ denotes all scenes that contain camouflaged objects. ‘ \uparrow / \downarrow ’ denotes that the higher/lower the score, the better. The 1st/2nd best results on column basis are indicated in red/blue.

| Methods | Overall | | | | Single-Obj | | | | Multi-Obj | | | |
|------------------------|----------------|---------------------|----------------------|----------------|----------------|---------------------|----------------------|----------------|----------------|---------------------|----------------------|----------------|
| | $S_m \uparrow$ | $\alpha E \uparrow$ | $F_\beta^w \uparrow$ | $M \downarrow$ | $S_m \uparrow$ | $\alpha E \uparrow$ | $F_\beta^w \uparrow$ | $M \downarrow$ | $S_m \uparrow$ | $\alpha E \uparrow$ | $F_\beta^w \uparrow$ | $M \downarrow$ |
| R2CNet-baseline [66] | 0.772 | 0.847 | 0.604 | 0.044 | 0.777 | 0.847 | 0.611 | 0.043 | 0.711 | 0.849 | 0.531 | 0.054 |
| R2CNet-RefT [66] | 0.806 | 0.878 | 0.668 | 0.037 | 0.810 | 0.880 | 0.674 | 0.035 | 0.753 | 0.870 | 0.607 | 0.046 |
| PFNet [37] | 0.791 | 0.876 | 0.651 | 0.040 | 0.795 | 0.876 | 0.656 | 0.039 | 0.740 | 0.868 | 0.594 | 0.051 |
| PFNet-RefT [66] [37] | 0.813 | 0.893 | 0.693 | 0.034 | 0.817 | 0.892 | 0.697 | 0.033 | 0.769 | 0.889 | 0.648 | 0.041 |
| PreyNet [64] | 0.806 | 0.890 | 0.690 | 0.034 | 0.811 | 0.892 | 0.696 | 0.033 | 0.749 | 0.878 | 0.618 | 0.042 |
| PreyNet-RefT [66] [64] | 0.816 | 0.901 | 0.705 | 0.033 | 0.821 | 0.900 | 0.710 | 0.032 | 0.759 | 0.902 | 0.648 | 0.041 |
| SINetV2 [8] | 0.813 | 0.874 | 0.678 | 0.036 | 0.818 | 0.874 | 0.684 | 0.035 | 0.763 | 0.864 | 0.615 | 0.045 |
| SINetV2-RefT [66] [8] | 0.822 | 0.887 | 0.696 | 0.033 | 0.827 | 0.888 | 0.702 | 0.032 | 0.766 | 0.866 | 0.629 | 0.043 |
| BSANet [70] | 0.818 | 0.893 | 0.702 | 0.034 | 0.823 | 0.895 | 0.707 | 0.033 | 0.766 | 0.873 | 0.643 | 0.041 |
| BSANet-RefT [66] [70] | 0.830 | 0.914 | 0.730 | 0.030 | 0.834 | 0.915 | 0.734 | 0.029 | 0.784 | 0.898 | 0.674 | 0.036 |
| BGNet [49] | 0.818 | 0.901 | 0.679 | 0.036 | 0.822 | 0.901 | 0.683 | 0.035 | 0.775 | 0.886 | 0.626 | 0.044 |
| BGNet-RefT [66] [49] | 0.840 | 0.912 | 0.739 | 0.029 | 0.844 | 0.914 | 0.745 | 0.028 | 0.791 | 0.888 | 0.677 | 0.038 |
| ZoomNet [40] | 0.813 | 0.884 | 0.688 | 0.032 | 0.818 | 0.885 | 0.695 | 0.031 | 0.747 | 0.870 | 0.605 | 0.042 |
| ZoomNet-RefT [66] [40] | 0.835 | 0.897 | 0.725 | 0.029 | 0.839 | 0.897 | 0.731 | 0.028 | 0.783 | 0.889 | 0.661 | 0.038 |
| DGNet [19] | 0.816 | 0.883 | 0.684 | 0.034 | 0.826 | 0.885 | 0.700 | 0.032 | 0.744 | 0.873 | 0.588 | 0.047 |
| DGNet-RefT [66] [19] | 0.824 | 0.891 | 0.701 | 0.032 | 0.830 | 0.892 | 0.709 | 0.031 | 0.745 | 0.873 | 0.596 | 0.046 |
| Our MLKG | 0.910 | 0.916 | 0.829 | 0.019 | 0.914 | 0.917 | 0.834 | 0.019 | 0.856 | 0.903 | 0.767 | 0.029 |

Table 4. Quantitative comparison on COD10K [8] dataset with the state-of-the-art COD methods. ‘ \uparrow / \downarrow ’ denotes that the higher/lower the score, the better. The 1st/2nd best results on column basis are indicated in red/blue.

| Method | $S_m \uparrow$ | $\alpha E \uparrow$ | $F_\beta^w \uparrow$ | $M \downarrow$ |
|-----------------|----------------|---------------------|----------------------|----------------|
| SINet [7] | 0.776 | 0.867 | 0.631 | 0.043 |
| C2FNet [48] | 0.813 | 0.886 | 0.686 | 0.036 |
| PFNet [37] | 0.800 | 0.868 | 0.660 | 0.040 |
| UGTR [56] | 0.818 | 0.850 | 0.667 | 0.035 |
| C2FNet-V2 [1] | 0.811 | 0.890 | 0.691 | 0.036 |
| TPRNet [65] | 0.817 | 0.869 | 0.683 | 0.036 |
| FAPNet [69] | 0.822 | 0.875 | 0.694 | 0.036 |
| BSANet [70] | 0.818 | 0.894 | 0.699 | 0.034 |
| BGNet [49] | 0.831 | 0.902 | 0.722 | 0.033 |
| FDNet [68] | 0.840 | 0.906 | 0.729 | 0.030 |
| SINetV2 [8] | 0.815 | 0.864 | 0.680 | 0.037 |
| PopNet [52] | 0.851 | 0.910 | 0.757 | 0.028 |
| CRNet [12] | 0.733 | 0.845 | 0.576 | 0.049 |
| PFNet+ [38] | 0.806 | 0.880 | 0.677 | 0.037 |
| DGNet [19] | 0.822 | 0.879 | 0.693 | 0.033 |
| DTINet [33] | 0.824 | 0.881 | 0.695 | 0.034 |
| CamoFormer [58] | 0.869 | 0.931 | 0.786 | 0.023 |
| HitNet [15] | 0.871 | 0.936 | 0.806 | 0.023 |
| Our MLKG | 0.910 | 0.916 | 0.829 | 0.019 |

our model exhibits obvious improvements when compared with the existing COD methods on R2C7K and COD10K.

4.5. Zero-Shot Generalization

The multi-level knowledge provides our model with extra rich domain knowledge, thus this helps our models to understand the unseen patterns. To assess the zero-shot generalization capability of our model, direct testing was conducted on three uni-modal COD datasets, *i.e.*, NC4K, CAMO, and CHAMELEON, without any adaptation training. We chose nine strong COD models as competitors. As reported in Table 5, our approach holds its own when compared to the COD methods fully-trained on each dataset, consistently achieving top-tier performance in most scenarios, frequently ranked the first or second position. While our method may not obtain the state-of-the-art on CAMO, it may need to consider the uncertainties caused by the dataset sizes (NC4K with 4121 images, CAMO with 250 images, and CHAMELEON with 76 images). Based on this phenomenon, we draw a conclusion that our designed multi-level knowledge empowers our model with robust zero-shot generalization capabilities.

4.6. Ablation Study

We designed a series of ablation experiments on R2C7K, to evaluate the effectiveness of each key component of our designed multi-level knowledge. As illustrated in Table 6, whether introducing **K#a**, **K#b**, or **K#c-K#g** individually, the rich knowledge derived from the MLLM significantly aids our model in achieving the more precise identification. Compared with **K#a**, **K#b** obtains better performance (see the second and third rows in Table 6), demonstrating the

Table 5. Our zero-shot performance against the fully-training results of the competitors on three COD datasets NC4K [34], CAMO [25], and CHAMELEON [8]. ‘ \uparrow / \downarrow ’ denotes that the higher/lower the score, the better. The 1st / 2nd best results on column basis are indicated in red/blue.

| Method | NC4K [34] | | | | CAMO [25] | | | | CHAMELEON [8] | | | |
|-----------------|----------------|---------------------|----------------------|----------------|----------------|---------------------|----------------------|----------------|----------------|---------------------|----------------------|----------------|
| | $S_m \uparrow$ | $\alpha E \uparrow$ | $F_\beta^w \uparrow$ | $M \downarrow$ | $S_m \uparrow$ | $\alpha E \uparrow$ | $F_\beta^w \uparrow$ | $M \downarrow$ | $S_m \uparrow$ | $\alpha E \uparrow$ | $F_\beta^w \uparrow$ | $M \downarrow$ |
| SINet [7] | 0.808 | 0.883 | 0.723 | 0.058 | 0.745 | 0.825 | 0.644 | 0.092 | 0.872 | 0.936 | 0.806 | 0.034 |
| C2FNet [48] | 0.838 | 0.901 | 0.762 | 0.049 | 0.796 | 0.865 | 0.719 | 0.080 | 0.886 | 0.933 | 0.825 | 0.033 |
| UR-COD [22] | 0.844 | 0.910 | 0.787 | 0.045 | 0.814 | 0.891 | 0.758 | 0.067 | 0.901 | 0.960 | 0.862 | 0.023 |
| C2FNet-V2 [1] | 0.840 | 0.900 | 0.770 | 0.048 | 0.799 | 0.869 | 0.730 | 0.077 | 0.893 | 0.947 | 0.845 | 0.028 |
| FAPNet [69] | 0.851 | 0.903 | 0.775 | 0.047 | 0.815 | 0.877 | 0.734 | 0.076 | 0.893 | 0.940 | 0.825 | 0.028 |
| BGNet [49] | 0.851 | 0.911 | 0.788 | 0.044 | 0.812 | 0.876 | 0.749 | 0.073 | 0.901 | 0.943 | 0.850 | 0.027 |
| SINetV2 [8] | 0.847 | 0.901 | 0.770 | 0.048 | 0.820 | 0.884 | 0.743 | 0.070 | 0.888 | 0.941 | 0.816 | 0.030 |
| DGNet [19] | 0.857 | 0.910 | 0.784 | 0.042 | 0.839 | 0.906 | 0.769 | 0.057 | 0.890 | 0.938 | 0.816 | 0.029 |
| CamoFormer [58] | 0.892 | 0.941 | 0.847 | 0.030 | 0.872 | 0.931 | 0.831 | 0.046 | 0.910 | 0.956 | 0.859 | 0.023 |
| Our MLKG | 0.900 | 0.918 | 0.833 | 0.036 | 0.828 | 0.877 | 0.744 | 0.075 | 0.935 | 0.941 | 0.875 | 0.020 |

Table 6. Ablation results on R2C7K [66] based on the model component and knowledge variants of our MLKG method. ‘ \uparrow / \downarrow ’ denotes that the higher/lower the score, the better. ‘VE’: Visual Encoder; ‘VD’: Visual Decoder; ‘KF’: Knowledge Factory; ‘KE’: Knowledge Encoder; ‘KI’: Knowledge Injector. ‘KF{K#a}’ denotes ‘Knowledge Factory produces knowledge K#a’. ‘KF{K#a-K#g}’ denotes ‘Knowledge Factory produces all seven kinds of knowledge K#a, K#b, ..., K#g’.

| Configurations | $S_m \uparrow$ | $\alpha E \uparrow$ | $F_\beta^w \uparrow$ | $M \downarrow$ |
|-------------------------|----------------|---------------------|----------------------|----------------|
| VE+VD | 0.895 | 0.888 | 0.788 | 0.023 |
| VE+VD+KF{K#a}+KE+KI | 0.904 | 0.916 | 0.819 | 0.020 |
| VE+VD+KF{K#b}+KE+KI | 0.906 | 0.914 | 0.822 | 0.020 |
| VE+VD+KF{K#c-K#g}+KE+KI | 0.906 | 0.914 | 0.818 | 0.020 |
| VE+VD+KF{K#a-K#g}+KE+KI | 0.910 | 0.916 | 0.829 | 0.019 |

effectiveness of comprehensible/rich natural language over abstract textual references. Furthermore, when simultaneously injecting knowledge from both camouflage-target and camouflaged-scene levels into our model, it helps our model to decompose the complex task of Ref-COD in a human-like way, resulting in enhanced overall performance.

4.7. Visualization

Figure 6 presents the qualitative comparison of our model with nine COD models. Compared with these strong competitors, our method achieves more accurate prediction masks. It is observed that our prediction masks present more subtle contour details of the targets, which are indistinguishable in the camouflaged scenes. This shows that our model understands the target object and the global scene in a more precise way. We would attribute this advantage to its mechanism of complex task decomposition and external knowledge injection.

5. Conclusion

This paper proposes a Multi-Level Knowledge-Guided (MLKG) multimodal method for Referring Camouflaged Object Detection (Ref-COD). The method leverages the semantic intelligence and intrinsic knowledge of Multi-modal Large Language Models (MLLMs) to decompose the complex task of Ref-COD in a human-like way. The MLKG method organizes multi-level knowledge descriptions from MLLMs to guide the segmentation model in perceiving camouflage-targets and camouflage-scene progressively while aligning textual references with camouflaged photos. The contributions of this paper include exploring the use of MLLMs for Ref-COD and COD, decomposing Ref-COD into two perspectives for better interpretability, and achieving state-of-the-art performance on the Ref-COD and COD benchmark. Additionally, the method demonstrates zero-shot generalization ability on uni-modal COD datasets due to the reasonable injection of rich knowledge.

We hope this work can provide a basis for future work in Ref-COD, COD, and even camouflaged vision perception, motivating the community toward complex pattern learning using large model knowledge.

6. Future Work

In our future efforts, we would try to extend this work mainly in the following three aspects.

(1) Future work can introduce more useful feature information into our current language-based knowledge structure, *e.g.*, latent knowledge from the hidden spaces of some models, structured knowledge from knowledge graphs. Moreover, it is necessary to consider incorporating other modalities, such as depth information and optical information, to further enhance the performance of Ref-COD. This can lead to more comprehensive and robust models that can handle diverse real-world scenarios.

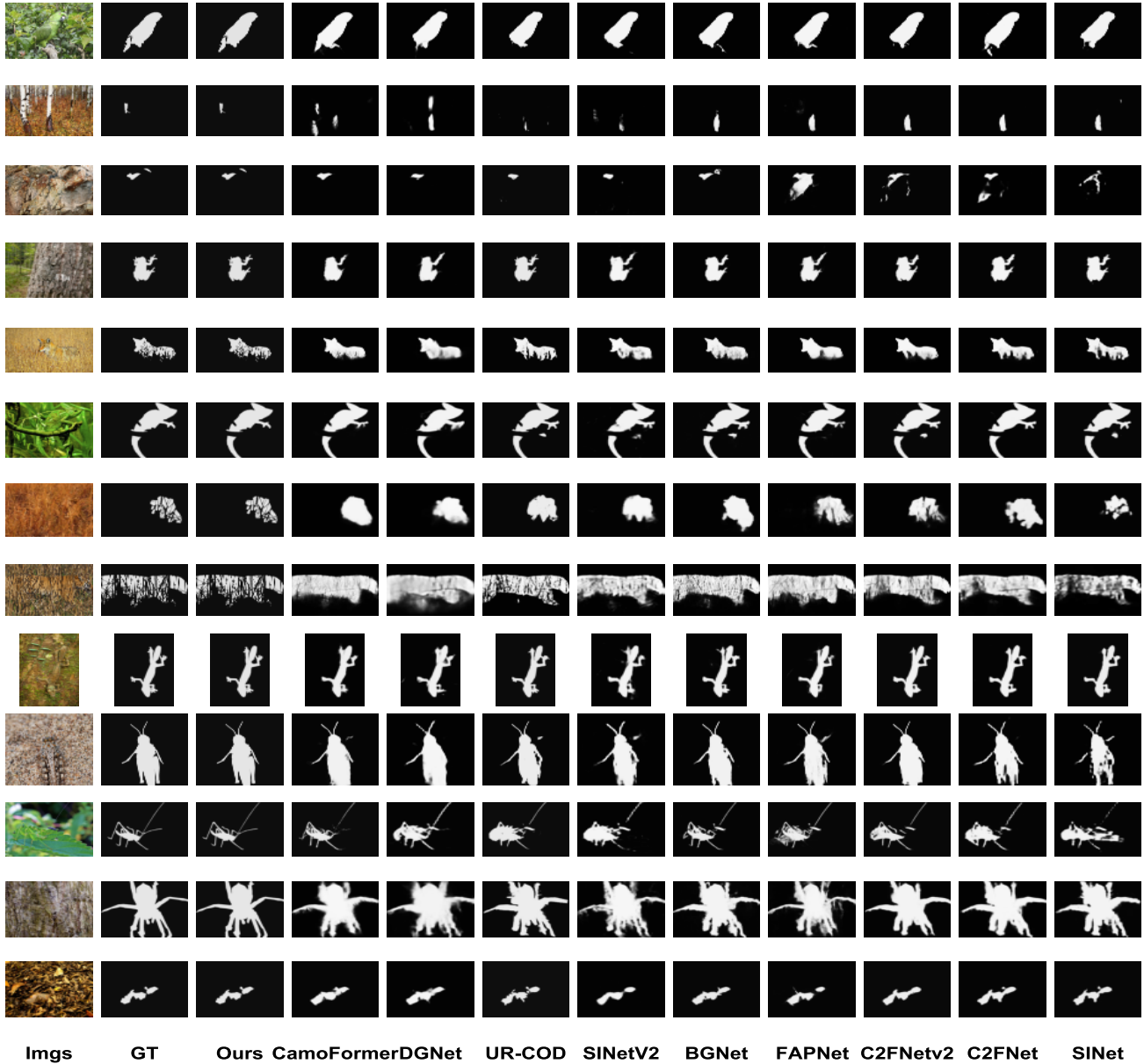


Figure 6. Visual comparison of the proposed method MLKG with nine strong COD methods. The first and second columns are camouflaged photos and their ground truth masks, respectively. Each of the remaining columns arranges the predictions of one method. The different shapes are due to the original different resolutions of these photos.

(2) The rapid development of Large Model brings more and more amazing features. Therefore, there is still room for further exploration of MLLMs for COD tasks. Future work can investigate how newly-updated sophisticated MLLMs can help provide even better performance and interpretability for COD.

(3) The proposed MLKG has been proven to be effective in Ref-COD, but the principle is universally applica-

ble. Future work can not only evaluate the performance of MLKG on more diverse and challenging datasets, but also focus on how to apply it to other visual and multimodal problems. This can help assess the generalization capability of the method and identify potential limitations or areas for improvement.

References

- [1] Geng Chen, Si-Jie Liu, Yu-Jia Sun, Ge-Peng Ji, Ya-Feng Wu, and Tao Zhou. Camouflaged object detection via context-aware cross-level fusion. *IEEE Transactions on Circuits and Systems for Video Technology*, 32(10):6981–6993, 2022. 7, 8
- [2] Tianshui Chen, Liang Lin, Riquan Chen, Yang Wu, and Xiaonan Luo. Knowledge-embedded representation learning for fine-grained image recognition. *arXiv preprint arXiv:1807.00505*, 2018. 3
- [3] Wenhu Chen, Hexiang Hu, Xi Chen, Pat Verga, and William W Cohen. Murag: Multimodal retrieval-augmented generator for open question answering over images and text. *arXiv preprint arXiv:2210.02928*, 2022. 3
- [4] Yuhao Cui, Zhou Yu, Chunqi Wang, Zhongzhou Zhao, Ji Zhang, Meng Wang, and Jun Yu. Rosita: Enhancing vision-and-language semantic alignments via cross-and intra-modal knowledge integration. In *Proceedings of the 29th ACM International Conference on Multimedia*, pages 797–806, 2021. 3
- [5] Deng-Ping Fan, Ming-Ming Cheng, Yun Liu, Tao Li, and Ali Borji. Structure-measure: A new way to evaluate foreground maps. In *Proceedings of the IEEE international conference on computer vision*, pages 4548–4557, 2017. 6
- [6] Deng-Ping Fan, Cheng Gong, Yang Cao, Bo Ren, Ming-Ming Cheng, and Ali Borji. Enhanced-alignment measure for binary foreground map evaluation. *arXiv preprint arXiv:1805.10421*, 2018. 6
- [7] Deng-Ping Fan, Ge-Peng Ji, Guolei Sun, Ming-Ming Cheng, Jianbing Shen, and Ling Shao. Camouflaged object detection. In *Proceedings of the IEEE/CVF conference on computer vision and pattern recognition*, pages 2777–2787, 2020. 3, 6, 7, 8
- [8] Deng-Ping Fan, Ge-Peng Ji, Ming-Ming Cheng, and Ling Shao. Concealed object detection. *IEEE transactions on pattern analysis and machine intelligence*, 44(10):6024–6042, 2021. 3, 6, 7, 8
- [9] Deng-Ping Fan, Ge-Peng Ji, Peng Xu, Ming-Ming Cheng, Christos Sakaridis, and Luc Van Gool. Advances in deep concealed scene understanding. *Visual Intelligence*, 1(1):16, 2023. 1, 3
- [10] Chunming He, Kai Li, Yachao Zhang, Longxiang Tang, Yulun Zhang, Zhenhua Guo, and Xiu Li. Camouflaged object detection with feature decomposition and edge reconstruction. In *CVPR*, pages 22046–22055, 2023. 3
- [11] Kaiming He, Xinlei Chen, Saining Xie, Yanghao Li, Piotr Dollár, and Ross Girshick. Masked autoencoders are scalable vision learners. In *Proceedings of the IEEE/CVF conference on computer vision and pattern recognition*, pages 16000–16009, 2022. 2
- [12] Ruozhen He, Qihua Dong, Jiaying Lin, and Rynson WH Lau. Weakly-supervised camouflaged object detection with scribble annotations. In *Proceedings of the AAAI Conference on Artificial Intelligence*, pages 781–789, 2023. 7
- [13] Dan Hendrycks and Kevin Gimpel. Gaussian error linear units (gelus). *arXiv preprint arXiv:1606.08415*, 2016. 5
- [14] Edward J Hu, Yelong Shen, Phillip Wallis, Zeyuan Allen-Zhu, Yuanzhi Li, Shean Wang, Lu Wang, and Weizhu Chen. Lora: Low-rank adaptation of large language models. *arXiv preprint arXiv:2106.09685*, 2021. 6
- [15] Xiaobin Hu, Shuo Wang, Xuebin Qin, Hang Dai, Wenqi Ren, Donghao Luo, Ying Tai, and Ling Shao. High-resolution iterative feedback network for camouflaged object detection. In *Proceedings of the AAAI Conference on Artificial Intelligence*, pages 881–889, 2023. 3, 7
- [16] Zhou Huang, Hang Dai, Tian-Zhu Xiang, Shuo Wang, Huai-Xin Chen, Jie Qin, and Huan Xiong. Feature shrinkage pyramid for camouflaged object detection with transformers. In *CVPR*, 2023. 3
- [17] Ge-Peng Ji, Guobao Xiao, Yu-Cheng Chou, Deng-Ping Fan, Kai Zhao, Geng Chen, and Luc Van Gool. Video polyp segmentation: A deep learning perspective. *Machine Intelligence Research*, 19(6):531–549, 2022. 1
- [18] Ge-Peng Ji, Lei Zhu, Mingchen Zhuge, and Keren Fu. Fast camouflaged object detection via edge-based reversible recalibration network. *PR*, 123:108414, 2022. 3
- [19] Ge-Peng Ji, Deng-Ping Fan, Yu-Cheng Chou, Dengxin Dai, Alexander Liniger, and Luc Van Gool. Deep gradient learning for efficient camouflaged object detection. *Machine Intelligence Research*, 20(1):92–108, 2023. 7, 8
- [20] Ge-Peng Ji, Deng-Ping Fan, Yu-Cheng Chou, Dengxin Dai, Alexander Liniger, and Luc Van Gool. Deep gradient learning for efficient camouflaged object detection. *MIR*, 20:92–108, 2023. 3
- [21] Ge-Peng Ji, Deng-Ping Fan, Peng Xu, Ming-Ming Cheng, Bowen Zhou, and Luc Van Gool. Sam struggles in concealed scenes—empirical study on ”segment anything”. *SCIENCE CHINA Information Sciences*, 66(12):226101, 2023. 2
- [22] Nobukatsu Kajiura, Hong Liu, and Shin’ichi Satoh. Improving camouflaged object detection with the uncertainty of pseudo-edge labels. In *ACM Multimedia Asia*, pages 1–7, 2021. 3, 8
- [23] Alexander Kirillov, Eric Mintun, Nikhila Ravi, Hanzi Mao, Chloe Rolland, Laura Gustafson, Tete Xiao, Spencer Whitehead, Alexander C Berg, Wan-Yen Lo, et al. Segment anything. *arXiv preprint arXiv:2304.02643*, 2023. 2, 3, 6
- [24] Takeshi Kojima, Shixiang Shane Gu, Machel Reid, Yutaka Matsuo, and Yusuke Iwasawa. Large language models are zero-shot reasoners. *Advances in neural information processing systems*, 35:22199–22213, 2022. 2
- [25] Trung-Nghia Le, Tam V Nguyen, Zhongliang Nie, Minh-Triet Tran, and Akihiro Sugimoto. Anabran network for camouflaged object segmentation. *Computer vision and image understanding*, 184:45–56, 2019. 3, 6, 8
- [26] Chen-Yu Lee, Saining Xie, Patrick Gallagher, Zhengyou Zhang, and Zhuowen Tu. Deeply-supervised nets. In *AISTATS*, pages 562–570. PMLR, 2015. 3
- [27] Mike Lewis, Yinhan Liu, Naman Goyal, Marjan Ghazvininejad, Abdelrahman Mohamed, Omer Levy, Ves Stoyanov, and Luke Zettlemoyer. Bart: Denoising sequence-to-sequence pre-training for natural language generation, translation, and comprehension. *arXiv preprint arXiv:1910.13461*, 2019. 2, 3

- [28] Aixuan Li, Jing Zhang, Yunqiu Lv, Bowen Liu, Tong Zhang, and Yuchao Dai. Uncertainty-aware joint salient object and camouflaged object detection. In *CVPR*, pages 10071–10081, 2021. 3
- [29] Haotian Liu, Chunyuan Li, Yuheng Li, and Yong Jae Lee. Improved baselines with visual instruction tuning. *arXiv preprint arXiv:2310.03744*, 2023. 2, 3
- [30] Haotian Liu, Chunyuan Li, Qingyang Wu, and Yong Jae Lee. Visual instruction tuning, 2023. 2, 3
- [31] Jiawei Liu, Jing Zhang, and Nick Barnes. Modeling aleatoric uncertainty for camouflaged object detection. In *WACV*, pages 1445–1454, 2022. 3
- [32] Liu Liu, Rujing Wang, Chengjun Xie, Po Yang, Fangyuan Wang, Sud Sudirman, and Wancai Liu. Pestnet: An end-to-end deep learning approach for large-scale multi-class pest detection and classification. *Ieee Access*, 7:45301–45312, 2019. 2
- [33] Zhengyi Liu, Zhili Zhang, Yacheng Tan, and Wei Wu. Boosting camouflaged object detection with dual-task interactive transformer. In *2022 26th International Conference on Pattern Recognition (ICPR)*, pages 140–146. IEEE, 2022. 7
- [34] Yunqiu Lv, Jing Zhang, Yuchao Dai, Aixuan Li, Bowen Liu, Nick Barnes, and Deng-Ping Fan. Simultaneously localize, segment and rank the camouflaged objects. In *Proceedings of the IEEE/CVF Conference on Computer Vision and Pattern Recognition*, pages 11591–11601, 2021. 3, 6, 8
- [35] Yunqiu Lv, Jing Zhang, Yuchao Dai, Aixuan Li, Nick Barnes, and Deng-Ping Fan. Towards deeper understanding of camouflaged object detection. *IEEE TCSVT*, 2023. 3
- [36] Ran Margolin, Lihi Zelnik-Manor, and Ayellet Tal. How to evaluate foreground maps? In *Proceedings of the IEEE conference on computer vision and pattern recognition*, pages 248–255, 2014. 6
- [37] Haiyang Mei, Ge-Peng Ji, Ziqi Wei, Xin Yang, Xiaopeng Wei, and Deng-Ping Fan. Camouflaged object segmentation with distraction mining. In *Proceedings of the IEEE/CVF Conference on Computer Vision and Pattern Recognition*, pages 8772–8781, 2021. 3, 7
- [38] H Mei, X Yang, Y Zhou, GP Ji, X Wei, and DP Fan. Distraction-aware camouflaged object segmentation. *SCIENTIA SINICA Informationis (SSI)*, 2023. 3, 7
- [39] Aditya Mogadala, Xiaoyu Shen, and Dietrich Klakow. Integrating image captioning with rule-based entity masking. *arXiv preprint arXiv:2007.11690*, 2020. 3
- [40] Youwei Pang, Xiaoqi Zhao, Tian-Zhu Xiang, Lihe Zhang, and Huchuan Lu. Zoom in and out: A mixed-scale triplet network for camouflaged object detection. In *Proceedings of the IEEE/CVF Conference on computer vision and pattern recognition*, pages 2160–2170, 2022. 3, 7
- [41] Adam Paszke, Sam Gross, Francisco Massa, Adam Lerer, James Bradbury, Gregory Chanan, Trevor Killeen, Zeming Lin, Natalia Gimelshein, Luca Antiga, et al. Pytorch: An imperative style, high-performance deep learning library. *Advances in neural information processing systems*, 32, 2019. 6
- [42] Federico Perazzi, Philipp Krähenbühl, Yael Pritch, and Alexander Hornung. Saliency filters: Contrast based filtering for salient region detection. In *2012 IEEE conference on computer vision and pattern recognition*, pages 733–740. IEEE, 2012. 6
- [43] Alec Radford, Jong Wook Kim, Chris Hallacy, Aditya Ramesh, Gabriel Goh, Sandhini Agarwal, Girish Sastry, Amanda Askell, Pamela Mishkin, Jack Clark, et al. Learning transferable visual models from natural language supervision. In *International conference on machine learning*, pages 8748–8763. PMLR, 2021. 3, 4, 6
- [44] Olaf Ronneberger, Philipp Fischer, and Thomas Brox. U-net: Convolutional networks for biomedical image segmentation. In *Medical Image Computing and Computer-Assisted Intervention—MICCAI 2015: 18th International Conference, Munich, Germany, October 5-9, 2015, Proceedings, Part III 18*, pages 234–241. Springer, 2015. 3
- [45] Krishna Kumar Singh, Santosh Divvala, Ali Farhadi, and Yong Jae Lee. Dock: Detecting objects by transferring common-sense knowledge. In *Proceedings of the European Conference on Computer Vision (ECCV)*, pages 492–508, 2018. 3
- [46] Wei Sun, Chengao Liu, Linyan Zhang, Yu Li, Pengxu Wei, Chang Liu, Jialing Zou, Jianbin Jiao, and Qixiang Ye. Dqnet: Cross-model detail querying for camouflaged object detection. *arXiv preprint arXiv:2212.08296*, 2022. 3
- [47] Yujia Sun, Geng Chen, Tao Zhou, Yi Zhang, and Nian Liu. Context-aware cross-level fusion network for camouflaged object detection. In *IJCAI*, pages 1025–1031, 2021. 3
- [48] Yujia Sun, Geng Chen, Tao Zhou, Yi Zhang, and Nian Liu. Context-aware cross-level fusion network for camouflaged object detection. *arXiv preprint arXiv:2105.12555*, 2021. 7, 8
- [49] Yujia Sun, Shuo Wang, Chenglizhao Chen, and Tian-Zhu Xiang. Boundary-guided camouflaged object detection. *arXiv preprint arXiv:2207.00794*, 2022. 3, 7, 8
- [50] Romal Thoppilan, Daniel De Freitas, Jamie Hall, Noam Shazeer, Apoorv Kulshreshtha, Heng-Tze Cheng, Alicia Jin, Taylor Bos, Leslie Baker, Yu Du, et al. Lamda: Language models for dialog applications. *arXiv preprint arXiv:2201.08239*, 2022. 2, 3
- [51] Jason Wei, Xuezhi Wang, Dale Schuurmans, Maarten Bosma, Fei Xia, Ed Chi, Quoc V Le, Denny Zhou, et al. Chain-of-thought prompting elicits reasoning in large language models. *Advances in Neural Information Processing Systems*, 35:24824–24837, 2022. 2
- [52] Zongwei Wu, Danda Pani Paudel, Deng-Ping Fan, Jingjing Wang, Shuo Wang, Cédric Demonceaux, Radu Timofte, and Luc Van Gool. Source-free depth for object pop-out. In *Proceedings of the IEEE/CVF International Conference on Computer Vision*, pages 1032–1042, 2023. 3, 7
- [53] Mochu Xiang, Jing Zhang, Yunqiu Lv, Aixuan Li, Yiran Zhong, and Yuchao Dai. Exploring depth contribution for camouflaged object detection. *arXiv preprint arXiv:2106.13217*, 2021. 3
- [54] Haozhe Xing, Yan Wang, Xujun Wei, Hao Tang, Shuyong Gao, and Wenqiang Zhang. Go closer to see better: Camouflaged object detection via object area amplification and figure-ground conversion. *IEEE TCSVT*, 2023. 3

- [55] Peng Xu, Xiatian Zhu, and David A Clifton. Multimodal learning with transformers: A survey. *IEEE Transactions on Pattern Analysis and Machine Intelligence*, 2023. 2
- [56] Fan Yang, Qiang Zhai, Xin Li, Rui Huang, Ao Luo, Hong Cheng, and Deng-Ping Fan. Uncertainty-guided transformer reasoning for camouflaged object detection. In *Proceedings of the IEEE/CVF International Conference on Computer Vision*, pages 4146–4155, 2021. 3, 7
- [57] Qinghao Ye, Haiyang Xu, Jiabo Ye, Ming Yan, Haowei Liu, Qi Qian, Ji Zhang, Fei Huang, and Jingren Zhou. mplug-owl2: Revolutionizing multi-modal large language model with modality collaboration. *arXiv preprint arXiv:2311.04257*, 2023. 3
- [58] Bowen Yin, Xuying Zhang, Qibin Hou, Bo-Yuan Sun, Deng-Ping Fan, and Luc Van Gool. Camoformer: Masked separable attention for camouflaged object detection. *arXiv preprint arXiv:2212.06570*, 2022. 7, 8
- [59] Bowen Yin, Xuying Zhang, Qibin Hou, Bo-Yuan Sun, Deng-Ping Fan, and Luc Van Gool. Camoformer: Masked separable attention for camouflaged object detection. *arXiv preprint arXiv:2212.06570*, 2023. 3
- [60] Jing Yu, Zihao Zhu, Yujing Wang, Weifeng Zhang, Yue Hu, and Jianlong Tan. Cross-modal knowledge reasoning for knowledge-based visual question answering. *Pattern Recognition*, 108:107563, 2020. 3
- [61] Jiahui Yu, Zirui Wang, Vijay Vasudevan, Legg Yeung, Mojtaba Seyedhosseini, and Yonghui Wu. Coca: Contrastive captioners are image-text foundation models. *arXiv preprint arXiv:2205.01917*, 2022. 3
- [62] Wenhao Yu, Chenguang Zhu, Zaitang Li, Zhiting Hu, Qingyun Wang, Heng Ji, and Meng Jiang. A survey of knowledge-enhanced text generation. *ACM Computing Surveys*, 54(11s):1–38, 2022. 3
- [63] Qiang Zhai, Xin Li, Fan Yang, Chenglizhao Chen, Hong Cheng, and Deng-Ping Fan. Mutual graph learning for camouflaged object detection. In *CVPR*, pages 12997–13007, 2021. 3
- [64] Miao Zhang, Shuang Xu, Yongri Piao, Dongxiang Shi, Shusen Lin, and Huchuan Lu. Preynet: Preying on camouflaged objects. In *Proceedings of the 30th ACM International Conference on Multimedia*, pages 5323–5332, 2022. 3, 7
- [65] Qiao Zhang, Yanliang Ge, Cong Zhang, and Hongbo Bi. Tprnet: camouflaged object detection via transformer-induced progressive refinement network. *The Visual Computer*, pages 1–15, 2022. 7
- [66] Xuying Zhang, Bowen Yin, Zheng Lin, Qibin Hou, Deng-Ping Fan, and Ming-Ming Cheng. Referring camouflaged object detection. *arXiv preprint arXiv:2306.07532*, 2023. 2, 6, 7, 8
- [67] Dehua Zheng, Xiaochen Zheng, Laurence T Yang, Yuan Gao, Chenlu Zhu, and Yiheng Ruan. Mffn: Multi-view feature fusion network for camouflaged object detection. In *WACV*, 2023. 3
- [68] Yijie Zhong, Bo Li, Lv Tang, Senyun Kuang, Shuang Wu, and Shouhong Ding. Detecting camouflaged object in frequency domain. In *Proceedings of the IEEE/CVF Conference on Computer Vision and Pattern Recognition*, pages 4504–4513, 2022. 3, 7
- [69] Tao Zhou, Yi Zhou, Chen Gong, Jian Yang, and Yu Zhang. Feature aggregation and propagation network for camouflaged object detection. *IEEE Transactions on Image Processing*, 31:7036–7047, 2022. 3, 7, 8
- [70] Hongwei Zhu, Peng Li, Haoran Xie, Xuefeng Yan, Dong Liang, Dapeng Chen, Mingqiang Wei, and Jing Qin. I can find you! boundary-guided separated attention network for camouflaged object detection. In *Proceedings of the AAAI Conference on Artificial Intelligence*, pages 3608–3616, 2022. 3, 7
- [71] Jinchao Zhu, Xiaoyu Zhang, Shuo Zhang, and Junnan Liu. Inferring camouflaged objects by texture-aware interactive guidance network. In *AAAI*, pages 3599–3607, 2021. 3
- [72] Mingchen Zhuge, Xiankai Lu, Yiyu Guo, Zihua Cai, and Shuhan Chen. Cubenet: X-shape connection for camouflaged object detection. *PR*, 127:108644, 2022. 3